Coherent Equalization and POLMUX-RZ-DQPSK for Robust 100-GE Transmission

Chris R. S. Fludger, Thomas Duthel, Dirk van den Borne, *Student Member, IEEE*, Christoph Schulien, *Member, IEEE*, Ernst-Dieter Schmidt, Torsten Wuth, *Member, IEEE*, Jonas Geyer, Erik De Man, Giok-Djan Khoe, *Fellow, IEEE, Senior Member, OSA*, and Huug de Waardt, *Member, IEEE*

***Abstract*—We discuss the use of a coherent digital receiver for the compensation of linear transmission impairments and polarization demultiplexing in a transmission system compatible with a future 100-Gb/s Ethernet standard. We present experimental results on the transmission performance of 111 Gbit/s POLMUX-RZ-DQPSK. For a dense WDM setup with channels carrying 111 Gbit/s with a 50 GHz channel spacing (2.0 bits/s/Hz), we show the feasibility of 2375 km transmission. This is enabled through coherent detection which results in excellent noise performance, and subsequent electronic equalization which provides the high tolerance to polarization mode dispersion and chromatic dispersion (CD). Furthermore, we discuss the impact of sampling and digital signal processing with either 1 or 2 samples/bit. We show that when combined with low-pass electrical filtering, 1 sample/bit signal processing is sufficient to obtain a large tolerance towards CD. The proposed modulation and detection techniques enable 111 Gbit/s transmission that is directly compatible with the existing 10 Gbit/s infrastructure.**

***Index Terms*—100 G Ethernet, 111 Gbit/s transmission, coherent detection, differential quadrature phase shift keying (DQPSK), electronic equalization, optical transmission, polarization multiplexing (POLMUX).**

I. Introduction

Optical networks designed for Ethernet traffic are becoming more important as the dominance of data over voice services increases. Work in both standards committees and research communities have targeted the transport of 100-Gbit/s Ethernet (100 GE) over wide area networks.

In recent years, a number of different alternatives have been proposed for single-wavelength 100-GE transport (>100 Gbit/s including forward error correction and Ethernet overhead). Ultra-high-frequency electronics has enabled the generation and detection of On-Off keyed (OOK) signals using electrical time-division multiplexing (ETDM) [1], [2] at 107 Gbit/s. Alternatively, return-to-zero differential quadrature phase shift keying (RZ-DQPSK) encodes 2 bits/symbol and has been demonstrated at ~50 Gbaud symbol rate [3], [4].

However, despite the excellent long-haul transmission performance of ~100 Gbit/s OOK or DQPSK modulation, significant challenges remain before single-wavelength 100-GE systems can be realized. For example, the introduction of electronic equalization for 10 Gbit/s systems has led to deployment over fiber with high polarization mode dispersion (PMD) [5], [6], and coarse control of chromatic dispersion (CD) throughout the link. This places a further burden on the development of 40 and 100 Gbit/s serial transmission systems, which are intrinsically more sensitive to fiber impairments.

One potential candidate to reduce the symbol rate even further and, therefore, improve the dispersion tolerance, is polarization multiplexing (POLMUX). This doubles the number of bits/symbol by transmitting independent information in each of the two orthogonal polarizations. POLMUX-RZ-DQPSK modulation therefore enables 111 Gbit/s transmission with only 27.75 Gsymbol/s by encoding 4 bits/symbol. This further increases the spectral efficiency and tolerance to CD and PMD, and places the symbol rate within reach of modern high-speed analogue-to-digital converters (ADCs) [5], facilitating the use of digital signal processing techniques. Coherent detection has recently received attention in the research community because of the potential to recover polarization multiplexed data [7], and correct linear distortions such as CD [8]–[10] and PMD [11], [12].

In this paper, we review the transmission capabilities of 111 Gbit/s POLMUX-RZ-DQPSK using coherent detection and electronic equalization. Simultaneous recovery of data on both polarizations is achieved using a polarization diverse intradyne coherent receiver. Clock and carrier recovery, polarization tracking and impairment mitigation are performed by digital signal processing based on twofold oversampled data. We show that such an approach is tolerant to CD, first-order PMD and strong optical filtering and achieves excellent transmission performance.

Using 27.75-Gbaud POLMUX-RZ-DQPSK and a digital coherent receiver, we demonstrate 10×111 Gbit/s DWDM transmission on a 50-GHz grid over 2375 km of SSMF. In addition, we emulate the strong optical filtering of 5 cascaded 50-GHz add-drop nodes using a wavelength selective switch (WSS). Furthermore, we show that a reduced complexity receiver, using only 1 sample/symbol signal processing can also result in a high tolerance to CD when low-pass electrical filtering is applied at the receiver.

Manuscript received July 13, 2007; revised October 18, 2007. This work was supported by the German government under the EIBONE project.

C. R. S. Fludger, T. Duthel, and C. Schulien are with CoreOptics GmbH, Nürnberg, Germany (e-mail: chris@coreoptics.com).

D. van den Borne, G.-D. Khoe, and H. de Waardt are with the COBRA Institute, Eindhoven University of Technology, 5600 MB Eindhoven, The Netherlands (e-mail: D.v.d.Borne@tue.nl).

E-D. Schmidt and E. De Man are with Nokia Siemens Networks GmbH & Co. KG, D-81379 Munich, Germany (e-mail: ernst-dieter.schmidt@nsn.com).

T. Wuth is with Siemens PSE GmbH & Co. KG, Munich, Germany (e-mail: torsten.wuth@siemens.com).

J. C. Geyer is with the Institute of Microwave Technology, University of Erlangen, Erlangen, Germany (e-mail: jonas@coreoptics.com).

Color versions of one or more of the figures in this paper are available online at http://ieeexplore.ieee.org.

Digital Object Identifier 10.1109/JLT.2007.912128

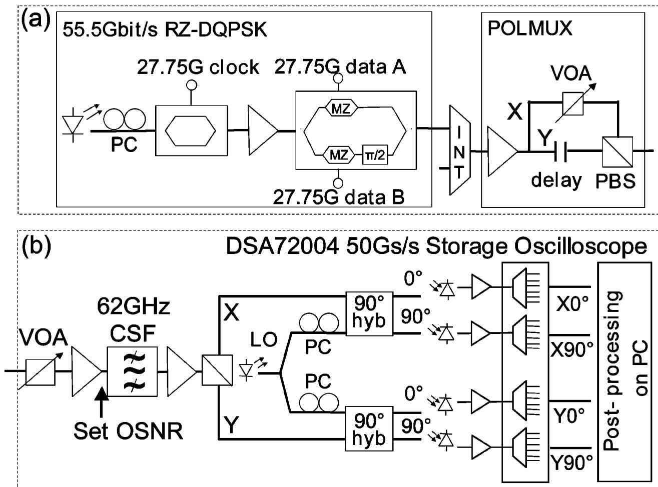

Fig. 1. Schematic of transmitter and receiver.

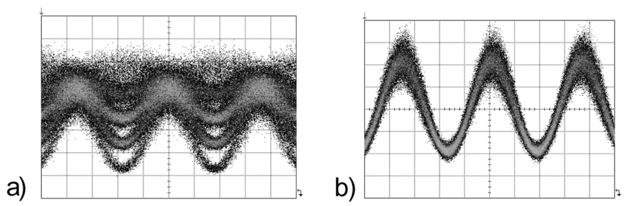

Fig. 2. Intensity eye diagrams for POLMUX-DQPSK (a) without and (b) with pulse carver.

This paper is organized as follows. In Section II we present the transmitter and receiver architecture while in Section III we review the signal processing algorithms. Back-to-back and linear impairment (CD, first-order PMD) measurements are shown in Section IV and the tolerance to narrow band optical filtering in Section V. An analysis of optimum electrical receive filters for 1 sample/bit signal processing is given in Section VI. The results of a longhaul DWDM transmission experiment are presented in Section VII. In Section VIII we summarise our conclusions.

II. Transmitter and Receiver Architecture

The experimental setup is shown in Fig. 1. The 111 Gbit/s POLMUX-RZ-DQPSK transmitter [Fig. 1(a)] consists of a pulse carver for RZ pulse carving, followed by a nested Mach-Zehnder (MZ) modulator for DQPSK modulation. The nested MZ modulator is driven by a 27.75-Gbit/s 2^{16} pattern, where both electrical drive signals (data A and B) are decorrelated by an 8 bit delay. Note that this decorrelation precisely results in a 4^8 pseudorandom quaternary sequence for proper modelling of the RZ-DQPSK modulation format. A 50-GHz interleaver with a 45-GHz 3-dB bandwidth is also included for later multichannel experiments. Finally, a polarization multiplexed signal is generated by dividing and recombining the signal with a 353 symbol delay using a polarization beam combiner. Fig. 2 shows NRZ and RZ directly detected eye diagrams for 111 Gbit/s POLMUX-RZ-DQPSK modulation.

The receiver [see Fig. 1(b)] composes of a polarization beam splitter (PBS), two fiber-based 90° hybrids, consisting of 3×3 couplers with a 2:2:1 splitting ratio [7], [13], and four single-ended Pin/TIA modules (U2T XPRV2022). To reduce the cost and complexity of the receiver, balanced detectors are not used and the distortion from directly detected components is minimized using a local oscillator (LO) to signal ratio of $\sim$18 dB. The absolute power on the photodetectors (dominated by the LO) was between $+1$ and -2 dBm, where the power variation was due to the use of an asymmetric 2:2:1 coupler. The input polarization state is not controlled, and an arbitrary mix of each transmitted polarization state is incident on the photodetectors. A tunable laser source (100 kHz linewidth) is used as a local oscillator, and is aligned to within 400 MHz of the transmit laser. Polarization controllers are required for the LO only because the receiver optics is not polarization maintaining. The photocurrents $(\mathrm{X}_0, \mathrm{X}_{90})$ from the X polarization photodetectors are given by [13]

$$\begin{pmatrix} X_0 \\ X_{90} \end{pmatrix} = \begin{pmatrix} 2 \\ 1 \end{pmatrix} \frac{|E_{\mathrm{LO}}|^2}{5} + \begin{pmatrix} 1 \\ 2 \end{pmatrix} \frac{|E_X|^2}{5} + \begin{pmatrix} \Re_e\{E_X E_{\mathrm{LO}}^*\} \\ \Im_m\{E_X E_{\mathrm{LO}}^*\} \end{pmatrix} \frac{2\sqrt{2}}{5} \tag{1}$$

where E_{LO} and E_{X} are the optical fields of the LO and signal on the X polarization, before the 90° hybrid. Similar expressions can be derived for the Y polarization. The first two terms represent noise terms due to the directly detected components. The directly detected LO can be removed using a D.C. block in front of the ADC, whilst the directly detected signal may be minimized by ensuring a high LO-signal ratio. The last term gives the real and imaginary part of the optical field of the signal, mixed to near-baseband by the LO.

Data sets of 21 μs are sampled at 50 Gs/s using a digital storage oscilloscope with 20-GHz electrical bandwidth (DSA72004, generously provided by Tektronix). The data is then postprocessed using a desktop PC. This allows the performance to be evaluated, and algorithms to be tested without the development of an expensive ASIC.

III. Digital Signal Processing and Electronic Equalization

The digital signal processing algorithms discussed in this section enable the compensation of transmission impairments and the recovery of polarization multiplexed data. Fig. 3 shows the different components of the signal processing, consisting of clock recovery and retiming, equalization, carrier recovery, slicer and digital decoder, and error-counting modules.

A. Clock Recovery and Retiming

The storage oscilloscope used in these experiments samples at 50 Gsamples/s. For a 27.75-Gbaud symbol rate, the stored data sequence has approximately 1.8 samples/bit and must be retimed to obtain an integer number of samples per bit (typically one or two). In a coherent receiver specifically designed for a 27.75–Gbaud symbol rate, the A/D converters (ADC) would sample at an exact multiple of the symbol rate such that only fine control of the clock timing is required.

First of all, in order to approximately resample the sequence to $\sim$2 samples/bit, the sampling rate is increased from 50 to 55.5 Gsymbol/s based on knowledge of the symbol rate and

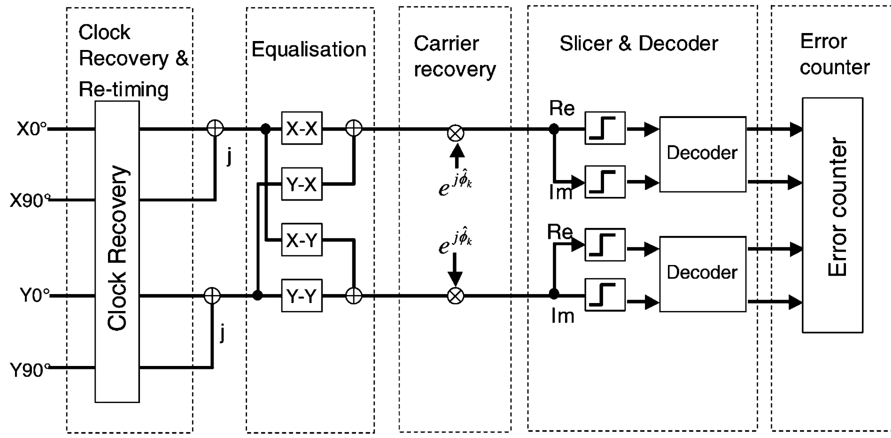

Fig. 3. Schematic of signal processing modules.

oscilloscope sampling rate. This typically leaves some residual timing offset caused by timing error and jitter that must be compensated using a clock-recovery scheme to resample to exactly 2 samples/bit. Here, we use a digital "filter and square" timing recovery [15] where the timing function is derived from the power envelope of the received signal

$$\chi = \frac{1}{2\pi} \arg\left(\sum_{n=mLN}^{(m+1)LM-1} P(n)e^{-j2\pi n/L}\right) \quad (2)$$

where m is the block index for blocks of length M, L is the oversampling factor and χ is a measure of the sampling phase error. The power envelope (P) is calculated from the square of the four received signal components $(X_0^2 + X_{90}^2 + Y_0^2 + Y_{90}^2)$. The sampling phase error is then used to resample the data using a cubic interpolator.

B. Equalizer

Electronic equalization is then used to compensate for linear transmission impairments and recover the polarization multiplexed data. The equalizer consists of four complex valued finite impulse response (FIR) filters, arranged in a butterfly structure (see Fig. 3) and optimized using a least-mean-squares (LMS) algorithm [16]. The output signals from the equalization stage (x' and y') at time k, are related to the input signal vectors ($\mathbf{x}$ and $\mathbf{y}$) containing samples $\mathrm{k - R + 1}$ to k by

$$x'(k) = \mathbf{h_{xx}} \cdot \mathbf{x}(k) + \mathbf{h_{yx}} \cdot \mathbf{y}(k) \quad (3)$$

$$y'(k) = \mathbf{h_{yy}} \cdot \mathbf{y}(k) + \mathbf{h_{xy}} \cdot \mathbf{x}(k) \quad (4)$$

where $\mathbf{h_{xx}}, \mathbf{h_{yx}}, \mathbf{h_{yy}}$, and $\mathbf{h_{xy}}$ are the T/2-spaced tap vectors, for the FIR filters, and "·" denotes the vector dot product. The length R of the tap vector is equal to the impulse response of the distortion that can be compensated. Initial equalizer acquisition is performed on the first 1000 symbols, which are subsequently discarded for error counting. The equalizer tap vectors are then updated continuously throughout the data set in order to track changes in the channel.

C. Carrier Recovery

In the next step, a carrier recovery stage corrects for the frequency and phase offset between the local oscillator and signal employing the "Viterbi-and-Viterbi" carrier phase estimation (CPE) method [17]. This uses a fourth power operation to remove the quaternary phase modulated data, whilst the estimated phase vector is calculated by averaging the complex phase vectors (x' or y') over multiple symbols $(2N + 1)$. The argument then gives the phase correction $(\hat{\phi}(k))$ that should be applied to symbol k:

$$\hat{\phi}(k) = \arg\left(\sum_{n=-N}^{N} x'^4(k+n)\right) \quad (5)$$

When amplified spontaneous emission (ASE) noise is the dominant impairment, N should be large so as to average the Gaussian noise and obtain a better phase estimate. In the presence of phase noise, induced through XPM impairments or from an LO with a broad linewidth (~MHz), a smaller number of symbols is preferable, so as to follow quick changes in phase. In our experiments, the optimum CPE length was found to be 17 symbols [22].

Although relatively narrow linewidth (~100 kHz) transmit and LO lasers were used in this work, simulations suggest that linewidths on the order of 1 MHz may be used with negligible OSNR penalty. It is also noted that the tolerance to frequency offsets between LO and signal (kept below 400 MHz in this work) could be improved using a separate frequency estimation and recovery algorithm [18].

D. Slicer & Decoder

A slicer then makes a digital decision on each symbol and differential decoding is used to avoid the possibility of cycle-slips. This doubles the bit-error ratio (BER) [23] resulting in ~0.5 dB OSNR penalty.

E. Error Counter

Finally, the differentially decoded sequence is compared to the transmitter PRBS sequence, taking into account the differential decoding. Errors are then counted for 524 288 symbols. For back-to-back measurements, the BER is measured at a

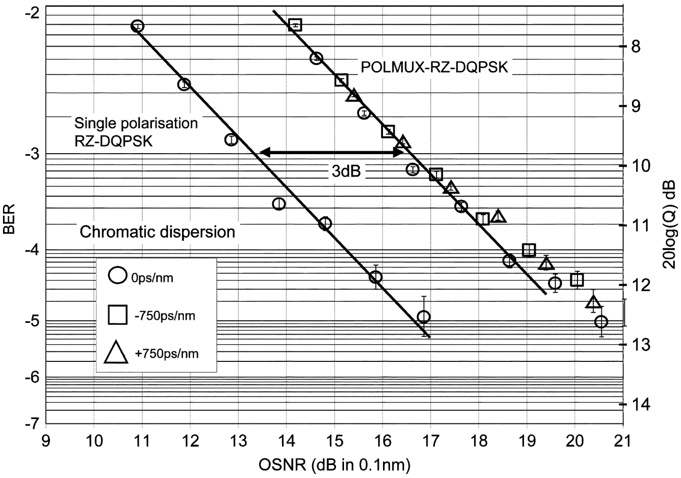

Fig. 4. Waterfall curves for single polarization and POLMUX-RZ-DQPSK with chromatic dispersion. Error bars are shown for 99% confidence.

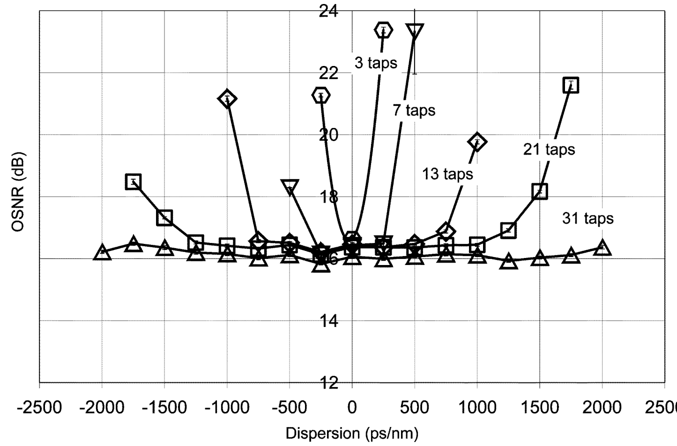

Fig. 5. OSNR for 10^{-3} BER vs chromatic dispersion for various tap lengths.

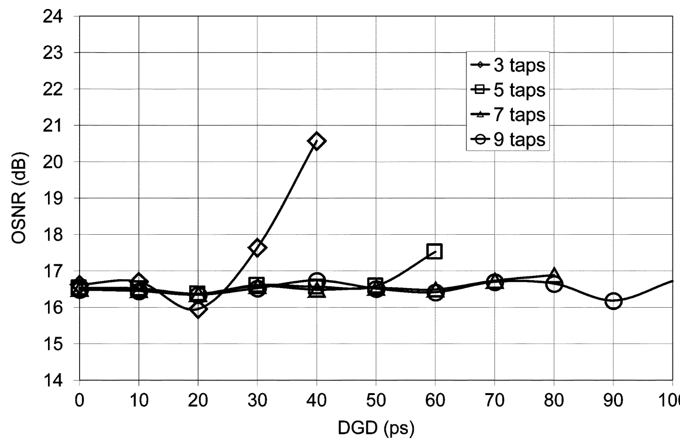

Fig. 6. OSNR for 10^{-3} BER vs DGD for various tap lengths.

number of different OSNR values, and the OSNR required for 10^{-3} BER is interpolated. For transmission measurements, 10 data sets are processed for each system configuration so that the average BER is based on 2×10^7 bits. The data sets are taken with a $\sim$1 minute interval and therefore have different input polarization and laser frequency offset. Note that because of the off-line processing used in this work, clock and equalizer acquisition must be performed independently on each data set.

IV. Linear Impairment Compensation

A. Back-to-Back OSNR Requirement

The back-to-back OSNR requirement for single-polarization RZ-DQPSK (55.5 Gbit/s) and POLMUX-RZ-DQPSK (111 Gbit/s) is depicted in Fig. 4. As expected, the doubling of the channel capacity results in a 3 dB OSNR penalty. For 111 Gbit/s POLMUX-RZ-DQPSK, a 16.5 dB OSNR is required for a BER of 10^{-3}. This is an improvement of 1.6 dB over previously reported 100 Gbit/s sensitivity measurements using 53 Gbaud RZ-DQPSK [4], or 4 dB for on-off keying with an optical equalizer [2].

B. Chromatic Dispersion Results

The chromatic dispersion tolerance of the receiver was measured using a combination of fiber spools and a tuneable dispersion compensator. In Fig. 4, the back-to-back OSNR requirement with $\pm$750 ps/nm chromatic dispersion is also shown. Since a coherent receiver is able to linearly detect the optical field, an FIR filter is able to accurately synthesize the inverse transfer functions required to compensate for linear fiber impairments such that little or no impairment is seen.

The OSNR requirement for 10^{-3} BER as a function of CD can be seen in Fig. 5 for different numbers of filter taps in the equalizer. This clearly shows that the CD tolerance is solely determined by the length of filter used in the equalizer [16]. For 31 taps, no significant penalty is evident for a dispersion window ranging from -2000 ps/nm to $+2000$ ps/nm. Reducing the number of FIR taps results directly in a decreased CD tolerance. However, even for 13 taps the CD tolerance is in excess of $\pm$750 ps/nm.

When one compares this tolerance to $\sim$ $\pm$8 ps/nm using 107 Gbit/s ETDM [2], or $\sim$ $\pm$25 ps/nm using 55.5 Gbaud RZ-DQPSK [3], the increased robustness is evident. Although this improvement is in part due to the lower symbol rate of POLMUX-RZ-DQPSK, the most significant contribution results from the coherent detection of the optical field, and the ability to synthesise the inverse of the quadratic phase response of the fiber using the FIR filters.

C. PMD Results

The PMD tolerance is also an important factor for optical transmission at ultra-high data rates. The tolerance to first order PMD or differential group delay (DGD) was measured using a birefringent element aligned at 45° to both polarization channels (worst-case alignment).

The DGD tolerance for various FIR filter tap lengths is shown in Fig. 6. Since DGD is a linear distortion in the optical field, and the complex envelope has been sampled for both polarization states, the inverse channel constructed by the FIR filters can effectively cancel the distortion induced through DGD. It can be seen that a 3 tap FIR filter is effective for DGD up to

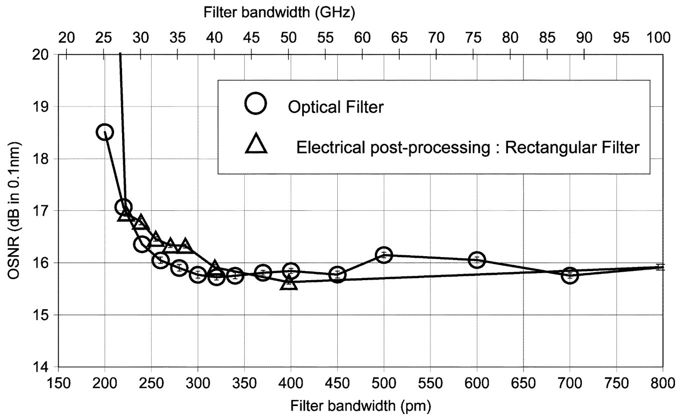

Fig. 7. OSNR required for 10^{-3} BER vs optical filter, or electrical postprocessed filter (2-sided) bandwidth.

30 ps, whilst a 9 tap FIR filter shows no penalty for a DGD of excess of 100 ps. Note that at 27.75 Gbaud, 100 ps is equivalent to 2.8 symbol periods. This DGD tolerance compares to $\sim$3 ps using 107 Gbit/s ETDM, or $\sim$6 ps using 55.5 Gbaud RZ-DQPSK [3]. Other demonstrations for 40 Gbit/s have shown that this coherent receiver structure is also effective for compensating CD and DGD together, and in addition, higher-order PMD [11], [12], [14].

V. Narrowband Optical Filtering Tolerance

Since most modern core optical networks are being designed for 10 Gbit/s data channels, based on a 50-GHz grid, it is desirable that 100 Gbit/s channels can be added with little or no change to the existing infrastructure. The tolerance with respect to narrowband optical filtering is shown in Fig. 7, and was measured using a NetTest X-Tract filter with a nearly rectangular passband.

27.75-Gbaud POLMUX-RZ-DQPSK requires only half the optical bandwidth of 55.5–Gbaud RZ-DQPSK and is, therefore, significantly more tolerant to strong optical filtering. To date, 55.5-Gbaud RZ-DQPSK and 107-Gbit/s ETDM have only been demonstrated on a 100- and 150-GHz WDM grid, respectively. In contrast, POLMUX-RZ-DQPSK can be deployed on a 50-GHz grid with little penalty. Even when the optical bandwidth is reduced further, for example through cascaded optical add-drop filtering, no significant penalty is evident until the 3-dB bandwidth drops below $\sim$30 GHz.

Since the electrical signal is proportional to the optical field after coherent detection, there should be equivalence between filtering in the optical and electrical domains. To investigate this, the data set recorded with a wide, 800-pm optical filter was digitally filtered using a variable bandwidth, infinite extinction rectangular filter. The resulting data was then processed using the algorithms described in Section III. This could also be implemented in hardware by using an analog low-pass filter, or low-bandwidth photoreceivers. Fig. 7 shows that the electrical filter tolerance (with a two-sided bandwidth) is almost identical to that of the optical filter.

VI. Reduced Complexity Receiver Using 1 Sample/Bit

ADCs sampling at up to 25 Gsamples/s are commercially available in 1st generation transponders incorporating digital signal processing at 10 Gbit/s [5]. ADCs at higher data-rates can be currently only found in state-of-the-art test-equipment. Besides the sample rate itself, the resolution of the ADC is also an important parameter to consider. Assuming that a digital coherent receiver requires 4 or 5 bits of vertical resolution, oversampling with 55.5 Gsamples/s on four input channels requires the processing of 880–1100 Gbits/s.

In the short-term, sampling with only 1 sample/bit would allow a receiver implementation with a lower complexity and less processing. On the other hand, the CD and DGD tolerance will be reduced since only T-spaced FIR filters can be used.

A T-spaced equalizer is not normally capable of compensating large amounts of CD, but when combined with an appropriate electrical low-pass filter at the receiver, a considerable tolerance can be obtained. By sampling with only 1 sample/bit, subsequent equalization is only able to operate on frequencies up to Nyquist frequency of $\sim$14 GHz. Energy content above this frequency is aliased, resulting in an OSNR penalty. A low-pass electrical filter can be used as an anti-aliasing filter before the ADC, to remove the distortion from the aliasing products and improve the effectiveness of the equalizer. Of course, excessive low-pass filtering will itself increases the intersymbol interference (ISI) resulting in an OSNR penalty as was shown in Section V. The equalizer must in turn compensate for both the additional ISI resulting from the low-pass filtering, and the channel distortions [19].

To illustrate this principle, the CD tolerance with a T-spaced equalizer has been computed in the following way: First, the data sets recorded on the oscilloscope ($\sim$2 samples/bit) are digitally filtered using a fifth-order $(\mathrm{d} = 5)$ super-Gaussian filter with normalized frequency response

$$H(\Omega) = \exp(-\ln(\sqrt{2})|\Omega|^{2d}) \tag{6}$$

The data is then resampled and requantized to emulate a 5 bit, 1 sample/bit ADC, which has approximately the same effective vertical resolution with which the data was originally sampled. This is intended to model the use of a realistic, albeit steep, low pass analogue anti-aliasing filter before a 1 sample/bit ADC. Requantization also limits the effectiveness of the subsequent equalizer to compensate for excessive low-pass filtering. The data is then passed through the receiver algorithms described in Section III, but now using only 1 sample/bit. Note that the sampling time instant has a large impact when using only 1 sample/bit, and is optimized to give the lowest mean-square error (MSE) at the output of the equalizer.

Fig. 8 shows the OSNR performance with $0, -250$ and -500 ps/nm CD with 1 sample/bit signal processing (13 tap FIR) and additional low-pass filtering (fifth-order super-Gaussian). Similar performance has also been achieved with shallower roll-off fifth-order Bessel [19] or Butterworth filters, where the optimum 3-dB bandwidth is decreased to provide good extinction above the Nyquist frequency. Although the performance becomes steadily worse when no CD is present and the electrical low-pass filtering bandwidth is reduced, the

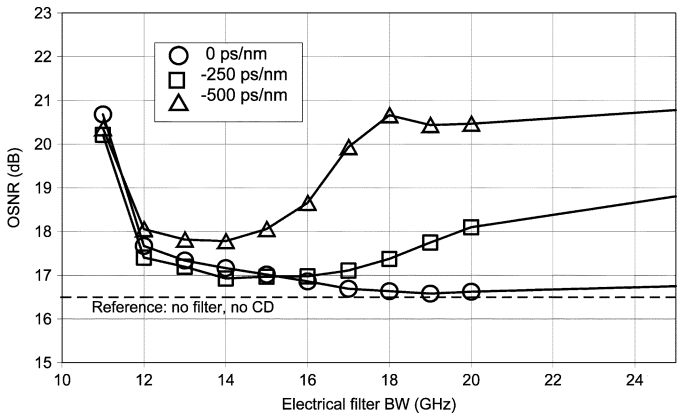

Fig. 8. OSNR versus electrical bandwidth (1-sided) using T-spaced equalization.

CD tolerance is improved. At a filtering bandwidth of 12 GHz and less, the performance both back-to-back and with dispersion quickly degrades since the equalizer is no longer able to compensate for the ISI created by excessive low-pass filtering. For 13 GHz low-pass filtering, there is $\sim$0.7 dB back-to-back penalty. At a CD of -500 ps/nm, the additional OSNR penalty is less than 0.8 dB. The 13-GHz low-pass filtering bandwidth has been subsequently used for 1 sample/bit transmission results in Section VII.

Not only do these results indicate that the dispersion tolerance using 1 sample/bit ADCs can be substantially improved by additional filtering, but also that lower bandwidth components can be used to reduce receiver cost and complexity.

VII. 111 Gbit/s Long-Haul Transmission Experiment

A. Experimental Setup

The transmitter was modified for a DWDM transmission experiment [(see Fig. 9(b)]. Odd and even transmitters modulate ten wavelength channels from an ECL laser array, which are then combined with a 50-GHz interleaver. All ten channels are then polarization multiplexed as before to create 111 Gbit/s POLMUX-RZ-DQPSK.

The transmitter output signal is predispersed using DCF with a -1530 ps/nm CD and launched into a recirculating loop consisting of 5×95 km standard fiber. The in-line under compensation per span equals -85 ps/nm. Hybrid EDFA-Raman amplifiers are used, where the distributed Raman amplification provided $\sim$14 dB on/off gain in the transmission fiber and improved the OSNR at the receiver. A loop synchronous polarization scrambler (LSPS) is used to reduce the loop-induced polarization effects, and a WSS with a 3 dB channel bandwidth of 43 GHz equalizes the power spectrum for each recirculation. The WSS also emulates the strong optical filtering of an optical add-drop node as can be found in agile optical networks. Note that the pass-bandwidth was $\sim$43 GHz irrespective of whether neighboring channels were turned on or off. After 5 recirculations, the received spectra of the signal had a bandwidth of 32 and 36.5 GHz (3 and 10 dB point, respectively). Postdispersion compensation fiber and a fiber-based tunable dispersion compensator (TDC) are used to set the net dispersion at the end of the link to near zero, or to explore the dispersion tolerance of the receiver. The optical spectrum after 2375 km is shown in Fig. 9(d). A channel selection filter (CSF) then selects the desired channel for measurement in the receiver. Ten data sets were processed for each system configuration so that the average BER is based on 2×10^7 bits.

B. Measurement Results and Discussion

Firstly, the BER performance of a centre channel at 1550.1 nm was optimized against channel launch power and transmission distance (see Fig. 10). As the transmission distance increases, the impact of nonlinearities increases which in turn decreases the optimum launch power from -4 dBm at 950 km to -6 dBm at 2850 km. It was further observed that the variance in BER between the ten measurement data sets increases at higher powers when the nonlinearity is most dominant. However, at the optimum launch power this variation is minimal, and a comparison of constellation diagrams (see Fig. 11) obtained for the back-to-back case and after 5 loops shows only a small amount of phase distortion resulting from nonlinear impairments along the transmission link. Both the use of Raman amplification and a POLMUX signal give rise to a lower optimum launch power. POLMUX signals typically suffer from cross-phase modulation between the orthogonally polarized signals at the same wavelength [20], whereas distributed Raman amplification leads to an increase in the path-averaged power [21]. However, the improved back-to-back performance from coherent detection and the robustness against linear channel distortions result in an overall better reach when compared to 55.5 Gbaud RZ-DQPSK or 107 Gb/s NRZ.

Fig. 12 shows the measured performance for all 10 wavelength channels after 1900 and 2375 km. All channels show a similar performance of between 1×10^{-4} and 5×10^{-4} BER. Hence, all measured channels have between 1 and 1.5 dB_Q margin at 2375 km with respect to the extended forward error correction (EFEC) limit.

By varying the postcompensation and the TDC, the tolerance to chromatic dispersion was measured after 2375 km (see Fig. 13). Using a 13 tap, T/2-spaced FIR filter, a tolerance window of 1500 ps/nm without penalty is observed. This is equal to the CD tolerance that was observed in the back-to-back measurement.

Next, the performance was evaluated using the 1 sample/bit signal processing presented in Section VI: First, the same data sets are digitally low-pass filtered with a 13-GHz fifth-order super-Gaussian, and afterwards requantized to emulate a 5-bit 1–sample/bit ADC. The data is then reprocessed with the equalization algorithms presented in Section III, using only 1 sample/bit. This emulates the use of an electrical anti-aliasing filter followed by a 1 sample/bit ADC. In Fig. 13 it can be seen that the low-pass filtering results in $\sim$0.5 dB_Q back-to-back penalty but achieves a CD tolerance window of $\sim$1000 ps/nm without a significant penalty. This shows that an early introduction of 100 GE receivers is possible using only 27.75 Gsample/s ADCs, providing 1 sample/bit.

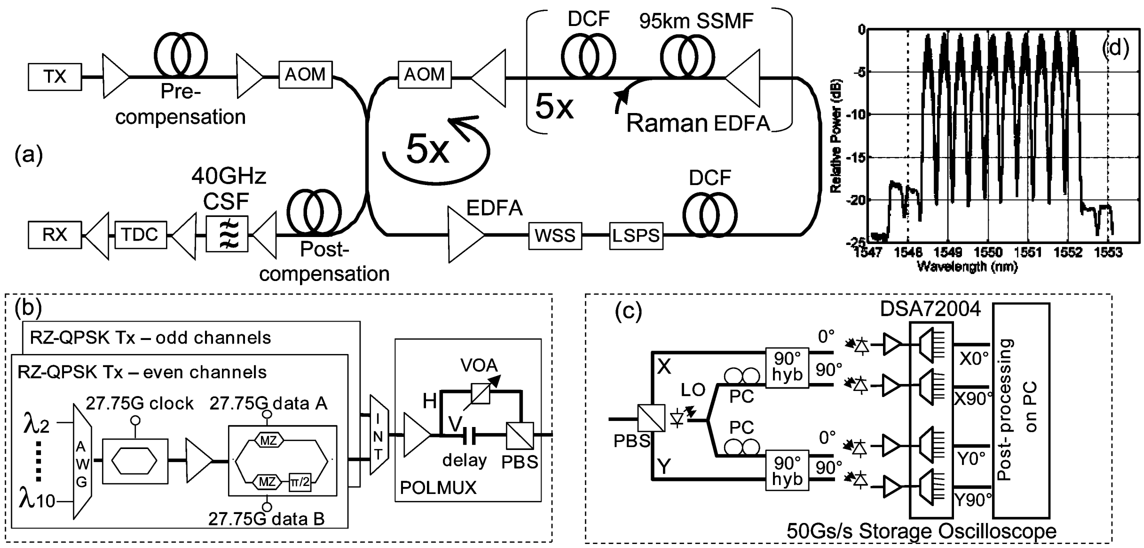

Fig. 9. Setup: (a) recirculating loop; (b) transmitter; (c) receiver; and (d) received optical spectrum.

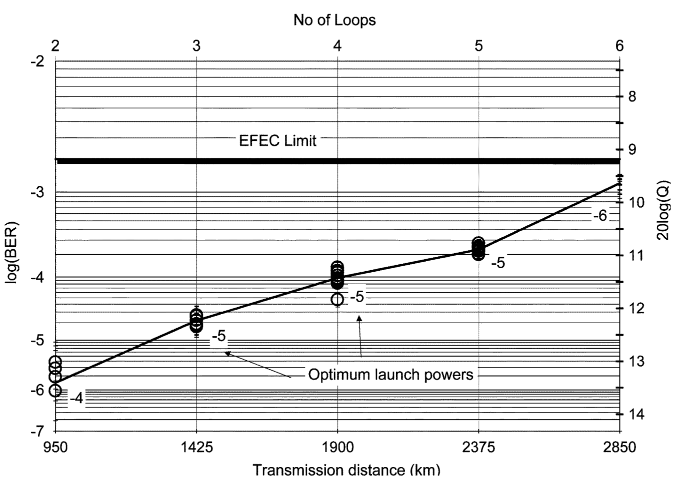

Fig. 10. BER versus distance and optimum launch power for centre channel.

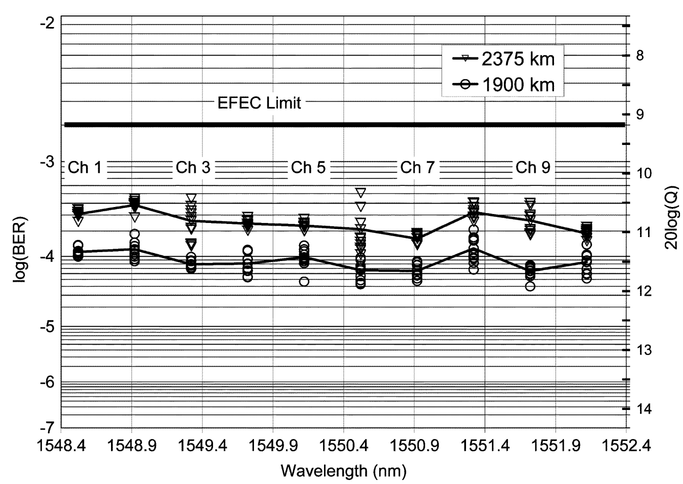

Fig. 12. BER for all ten channels after 1900 and 2375 km. Dots show measurement sets (2×10^6 bits) and lines show average (2×10^7 bits).

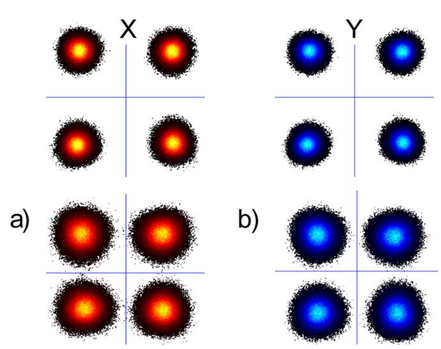

Fig. 11. Constellation diagrams for X and Y polarizations: (a) back-to-back (25 dB OSNR); (b) after 2375 km, BER $\sim 2 \times 10^{-4}$.

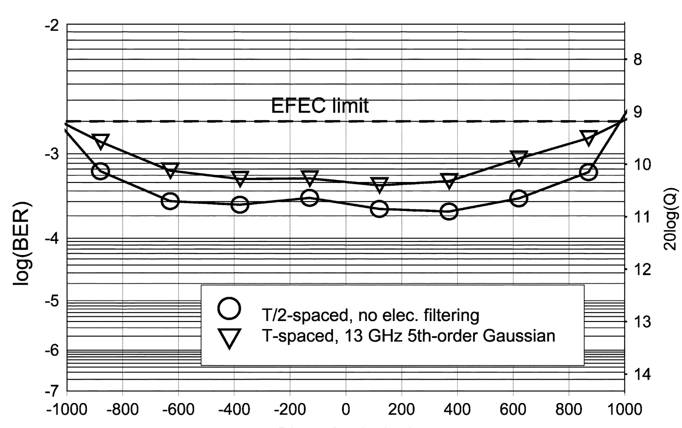

Fig. 13. Average BER versus residual chromatic dispersion after 2375 km transmission. Results shown for 13 tap T/2-spaced equalizer, and a T-spaced equalizer with additional electrical filtering.

The presented results show the opportunity to use 111 Gbit/s transmitters and receivers on network infrastructure that has been designed for 10 Gbit/s systems, without the use of an optical TDC or optical PMD compensator.

VIII. Conclusion

We have successfully demonstrated the use of 27.75 Gbaud POLMUX-RZ-DQPSK for the transport of 100 Gbit/s payloads. The high spectral efficiency achievable with POLMUX-RZ-DQPSK modulation makes it ideal for use on existing 10 Gbit/s infrastructure with 50-GHz channel spacing and multiple add-drop nodes.

We have shown 1 Tbit/s DWDM transmission (2.0 b/s/Hz) of ten 111 Gbit/s data channels over 2375 km standard fiber and have emulated the strong optical filtering from five add-drop nodes. We have shown that using T/2-spaced signal processing, a nearly arbitrary amount of CD and DGD can be compensated. Furthermore, when only T-spaced processing is realizable, the use of additional electrical filtering results in a large dispersion tolerance of over 1000 ps/nm after transmission. This facilitates an early introduction of coherent equalization for 100 GE, using ADCs that only need to sample at 1 sample/bit.

References

[1] J. H. Sinksy, A. Adamiecki, L. Buhl, G. Raybon, P. Winzer, O. Wohlgemuth, M. Duelk, C. R. Doerr, A. Umbach, H.-G. Bach, and D. Schmidt, "107-Gbit/s opto-electronic receiver with hybrid integrated photodetector and demultiplexer," in *Proc. OFC2007*, Anaheim, CA, 2007, Paper PDP30.

[2] P. J. Winzer, G. Raybon, C. R. Doerr, M. Duelk, and C. Dorrer, "107-Gb/s optical signal generation using electronic time-division multiplexing," *J. Lightw. Technol.*, vol. 24, no. 8, Aug. 2006.

[3] M. Daikoku, I. Morita, H. Taga, H. Tanaka, T. Kawanishi, T. Sakamoto, T. Miyazaki, and T. Fujita, "100-Gb/s DQPSK transmission experiment without OTDM for 100G ethernet transport," *J. Lightw. Technol.*, vol. 25, no. 1, Jan. 2007.

[4] P. J. Winzer, G. Raybon, C. R. Doerr, L. L. Buhl, T. Kawanishi, T. Sakamoto, M. Izutsu, and K. Higuma, "2000-km WDM Transmission of 10 × 107-Gb/s RZ-DQPSK," in *Proc. ECOC2006*, Cannes, France, 2006, Paper Th4.1.3.

[5] A. Färbert, S. Langenbach, N. Stojanovic, C. Dorschky, T. Kupfer, C. Schulien, J.-P. Elbers, H. Wernz, H. Griesser, and C. Glingener, "Performance of a 10.7 Gb/s receiver with digital equalizer using maximum likelihood sequence estimation," in *Proc. ECOC2004*, Stockholm, Sweden, 2004, Paper PD-Th4.1.5.

[6] T. Kupfer, J. Whiteaway, and S. Langenbach, "PMD compensation using electronic equalization particular maximum likelihood sequence estimation," in *Proc. OFC2007*, Anaheim, CA, 2007, Paper OMH1.

[7] S. J. Savory, A. D. Stewart, S. Wood, G. Gavioli, M. G. Taylor, R. I. Killey, and P. Bayvel, "Digital equalisation of 40 Gbit/s per wavelength transmission over 2480 km of standard fibre without optical dispersion compensation," in *ECOC 2006*, 2006, Paper Th2.5.5.

[8] D.-S. Ly-Gagnon, S. Tsukamoto, K. Katoh, and K. Kikuchi, "Coherent detection of optical quadrature phase-shift keying signals with carrier phase estimation," *J. Lightw. Technol.*, vol. 24, no. 1, Jan. 2006.

[9] B. Spinnler, P. M. Krummrich, and E.-D. Schmidt, "Chromatic dispersion tolerance of coherent optical communications systems with electrical equalization," in *Proc. OFC2006*, 2006, Paper OWB2.

[10] M. G. Taylor, "Coherent detection method using DSP for demodulation of signal and subsequent equalization of propagation impairments," *IEEE Photon. Technol. Lett.*, vol. 16, no. 2, Feb. 2004.

[11] G. Charlet, J. Renaudier, M. Salsi, H. Mardoyan, P. Tran, and S. Bigo, "Efficient mitigation of fiber impairments in an ultra-long haul transmission of 40 Gbit/s polarization-multiplexed data, by digital processing in a coherent receiver," in *OFC2007*, Mar. 2007, Paper PDP17.

[12] C. Laperle, B. Villeneuve, Z. Zhang, D. McGhan, H. Sun, and M. O'Sullivan, "Wavelength division multiplexing (WDM) and polarization mode dispersion (PMD) performance of a coherent 40 Gbit/s dual-polarization quadrature phase shift keying (DP-QPSK) transceiver," in *Proc. OFC2007*, Anaheim, CA, 2007, Paper PDP16.

[13] P. J. Anslow, C. R. S. Fludger, S. Savory, I. Hardcastle, and J. Fells, "Frequency selective coherent receiver for agile networks," in *ECOC2006*, Cannes, France, 2006, Paper Mo4.2.4.

[14] D. van den Borne, T. Duthel, C. R. S. Fludger, E. D. Schmidt, T. Wuth, C. Schulien, E. Gottwald, G. D. Khoe, and H. de Waardt, "Electrical PMD compensation in 43-Gb/s POLMUX-NRZ-DQPSK enabled by coherent detection and equalization," in *Proc. ECOC2007*, Berlin, Sep. 2007, Paper 8.3.1.

[15] J. W. M. Bergmans, *Digital Baseband Transmission and Recording*. Boston, MA: Kluwer Academic, 1996.

[16] S. J. Savory, G. Gavioli, R. I. Killey, and P. Bayvel, "Transmission of 42.8 Gbit/s polarization multiplexed NRZ-QPSK over 6400 km of standard fiber with no optical dispersion compensation," in *Proc. OFC2007*, Anaheim, CA, 2007, Paper OTUA1.

[17] A. J. Viterbi and A. M. Viterbi, "Nonlinear estimation of PSK-Modulated carrier phase with application to burst digital transmission," *IEEE Trans. Inf. Theory*, vol. IT-29, no. 4, Jul. 1983.

[18] A. Leven, "Frequency estimation in intradyne reception," *IEEE Photon. Technol. Lett.*, vol. 19, no. 6, Mar. 15, 2007.

[19] T. Duthel, C. R. S. Fludger, D. van den Borne, C. Schulien, E.-D. Schmidt, T. Wuth, E. de Man, G.-D. Khoe, and H. de Waardt, "Impairment tolerance of 111 Gbit/s POLMUX-RZ-DQPSK using a reduced complexity coherent receiver with a Tspaced equalizer," in *Proc. ECOC2007*, Berlin, Germany, Sep. 2007, Paper Mo.1.3.3.

[20] G. P. Agrawal, *Nonlinear Fiber Optics*, 2nd ed. New York: Academic, 1995, pp. 243–247, ISBN 0-12-045142-5.

[21] M. N. Islam, *Raman Amplifiers for Telecommunications 2*. New York: Springer, 2004, pp. 603–611.

[22] D. van den Borne, T. Duthel, C. R. S. Fludger, E.-D. Schmidt, T. Wuth, C. Schulien, E. Gottwald, G. D. Khoe, and H. de Waardt, "Carrier phase estimation for coherent equalization of 43-Gb/s POLMUX-NRZ-DQPSK transmission with 10.7 Gb/s NRZ neighbours," in *Proc. ECOC2007*, Berlin, Germany, Sep. 2007, Paper 7.2.3.

[23] J. G. Proakis, *Digital Communications*, 4th ed. New York: McGraw-Hill, 2000, pp. 271–272.

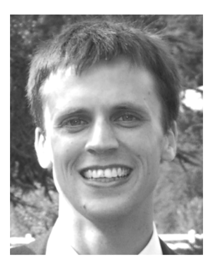

Chris R. S. Fludger was born in Beckenham, U.K, on March 12, 1975. He received the M.Eng. degree with distinction, and the Ph.D. degree in electronic engineering from Cambridge University, Cambridge, U.K.

In 1998, he joined Nortel Networks Research Laboratories, Harlow, U.K., where he worked on electronic signal processing, advanced optical modulation techniques and Raman amplification. He is currently with CoreOptics in Germany, developing next generation 10G, 40G, and 100G optical transmission modules for open tolerant networks.

Dr. Fludger is a Chartered Engineer and member of the Institute of Engineering and Technology.

Thomas Duthel was born in Germany in 1976. He received the Dipl.-Ing. (FH) degree in electrical engineering/telecommunication from Flensburg University of Applied Science, Germany, in 2000 and the Dr.-Ing. degree from Technische Universität Dresden, Germany, in 2005.

While working towards the Ph.D. degree, his main research interest was the synthesis and manufacturing of fiber optical dispersion compensators for high-speed optical transmission systems. He is currently with CoreOptics, Nuremburg, Germany, on advanced modulation formats for 40 and 100 Gbit/s optical transmission over existing network infrastructure.

Dirk van den Borne (S'04) was born in Bladel, The Netherlands, on October 7, 1979. He received the M.Sc. degree (*cum laude*) in electric engineering from Eindhoven University of Technology, Eindhoven, The Netherlands, in 2004.

He was with Fuijtsu Laboratories Ltd., Kawasaki, Japan, and Siemens AG, Munich. Currently, he is working toward the Ph.D. degree at Eindhoven University of Technology in collaboration with Nokia Siemens Networks (previously Siemens AG), Munich. His focus is on improving long-haul transmission systems using robust modulation formats and electronic impairment mitigation. He has authored and coauthored more than 50 refereed papers and conference contributions.

Mr. van den Borne received the KIVI-NIRIA telecommunication award and the IEEE-LEOS graduate student fellowship in 2007.

Christoph Schulien (M'97) was born in Germany in 1959. He received the Dipl.-Ing. degree in electrical engineering and the Dr.-Ing. degree, both from the University of the Saarland, Saarbrücken, Germany, in 1986 and 1992, respectively.

He began his career with Philips Kommunikations Industrie (PKI), Nuremberg, Germany, in 1992 in the field of high-speed mixed-signal circuit design for optical communications. Following the acquisition of PKI by Lucent Technologies, he headed the design and integration of 2.5 and 10 Gb/s interface modules to Lucent's Wavestar DWDM product portfolio. Subsequently, he led the high-speed technology development team for Lucent Technologies' first generation 40 Gb/s program. In early 2001, he cofounded CoreOptics, Nuremberg, where he contributed to the growth of the company in various management positions both on the technical as well as the business front. Most recently, he assumed responsibility for CoreOptics' next generation 40 and 100 Gb/s development programs. His particular interest is in advanced modulation formats and digital signal processing concepts for open tolerant networks.

Dr. Schulien is a member of the IEEE Communications Society.

Ernst-Dieter Schmidt, photograph and biography not available at the time of publication.

Torsten Wuth (M'05) was born in Germany in 1971. He received the Diploma degree in electrical engineering from the University of Dortmund, Dortmund, Germany, and the Doctoral degree from the Christian-Albrechts University at Kiel, Germany.

After a Postdoctoral period with the Chalmers University of Technology, Gothenburg, Sweden, he joined CoreOptics, Nuremberg, Germany. He is currently with Siemens PSE working on advanced transmission technologies for next generation networks at Nokia Siemens Networks, Munich, Germany.

Dr. Wuth is a member of the Alpenverein.

Jonas Geyer was born in Germany in 1982. He received the Dipl.-Ing. degree with distinction in electrical engineering from Friedrich-Alexander-University of Erlangen-Nuremberg, Germany in 2007.

He is working toward the Ph.D. degree in collaboration with CoreOptics, Nuremberg, on advanced modulation formats and signal processing in next generation optical transmission systems.

Erik De Man, photograph and biography not available at the time of publication.

Giok-Djan Khoe (S'71–M'71–SM'85–F'91) received the degree of Ingenieur in electrical engineering (*cum laude*) from the Eindhoven University of Technology, Eindhoven, The Netherlands, in 1971.

He began his research with the Dutch Foundation for Fundamental Research on Matter (FOM) Laboratory on Plasma Physics, Rijnhuizen. In 1973, he joined Philips Research Laboratories to work in the area of optical fiber communication systems. He became a full professor with Eindhoven University of Technology in 1994. Most of his work has been devoted to optical fiber systems and components. He has more than 40 U.S. Patents and has authored and coauthored more than 300 papers, invited papers, and book chapters.

Dr. Khoe has been a Fellow of the Optical Society of America (OSA) since 2006 and received the MOC/GRIN (Mirco-Optics/Graded-Index) award in 1997. His professional activities include many conferences, where he has served on technical committees, management committees, and advisory committees as a member or chairman. He has been involved in journal activities, as associate editor, as a member of the advisory board or as reviewer. His has served in the IEEE/LEOS organization as President and in many other ways.

Huug de Waardt (M'05) was born in Voorburg, The Netherlands, in December 1953. He received the M.Sc.E.E. and the Ph.D. degrees from the Delft University of Technology, The Netherlands, in 1980 and 1995, respectively.

In 1981, he began his professional carrier in the Physics Department at PTT Research, Leidschendam, The Netherlands, where he worked on the performance issues of optoelectronic devices. In 1989, he moved to the Transmission Department and became involved in WDM high-bit-rate optical transmission. In 1995, he was appointed Associated Professor with the Eindhoven University of Technology (TU/e), Eindhoven, The Netherlands, in the area of high-capacity trunk transmission. He coordinated the participation of TU/e in ACTS Upgrade, ACTS BLISS, ACTS APEX, and IST FASHION. Presently, he serves as project leader of the national research initiative Freeband Broadband Photonics (2004–2008). His current interests are in high capacity optical transmission and networking, integrated optics, and semiconductor optical amplifiers/modulators. He (co)authored more than 150 conference and journal papers.